

# Anti-PSMA/CD3 Bispecific Antibody Delivery and Antitumor Activity Using a Polymeric Depot Formulation

Wilhem Leconet<sup>1</sup>, He Liu<sup>1</sup>, Ming Guo<sup>1</sup>, Sophie Le Lamer-Déchamps<sup>2</sup>, Charlotte Molinier<sup>2</sup>, Sae Kim<sup>1</sup>, Tjasa Vrlic<sup>2</sup>, Murielle Oster<sup>2</sup>, Fang Liu<sup>2</sup>, Vicente Navarro<sup>1</sup>, Jaspreet S. Batra<sup>1</sup>, Adolfo Lopez Noriega<sup>2</sup>, Sylvestre Grizot<sup>2</sup>, and Neil H. Bander<sup>1</sup>



## Abstract

Small therapeutic proteins represent a promising novel approach to treat cancer. Nevertheless, their clinical application is often adversely impacted by their short plasma half-life. Controlled long-term delivery of small biologicals has become a challenge because of their hydrophilic properties and in some cases their limited stability. Here, an *in situ* forming depot-injectable polymeric system was used to deliver Bij591, a bispecific T-cell engager (BiTE) targeting both prostate-specific membrane antigen (PSMA) and the CD3 T-cell receptor in prostate cancer. Bij591 induced T-cell activation, prostate cancer-directed cell lysis, and tumor growth inhibition. The use of diblock (DB) and triblock (TB) biodegradable polyethylene glycol-poly(lactic acid;

PEG-PLA) copolymers solubilized in tripropionin, a small-chain triglyceride, allowed maintenance of Bij591 stability and functionality in the formed depot and controlled its release. In mice, after a single subcutaneous injection, one of the polymeric candidates, TB1/DB4, provided the most sustained release of Bij591 for up to 21 days. Moreover, the use of Bij591-TB1/DB4 formulation in prostate cancer xenograft models showed significant therapeutic activity in both low and high PSMA-expressing tumors, whereas daily intravenous administration of Bij591 was less efficient. Collectively, these data provide new insights into the development of controlled delivery of small therapeutic proteins in cancer. *Mol Cancer Ther*; 17(9): 1927–40. ©2018 AACR.

## Introduction

Antibodies are today among the most attractive cancer therapeutic agents due to their target specificity, but also for their ability to be engineered, improving their cytotoxic properties against the targeted cancer cells (1, 2). Among these antibody-based drugs, bispecific antibodies can engage two targets simultaneously, the second antigen can be either tumor specific or from another cell type (3). There are two bispecific antibodies that have been approved in the clinic, blinatumomab and catumaxomab (discontinued in 2014 for commercial reasons), which have the ability to target a cancer cell marker (CD19 and EpCAM, respectively) and CD3, a T-cell coreceptor well-known to activate and promote T-cell killing of tumor cells (4, 5). These recombinant antibodies act as a bridge to create an immune synapse and retarget immune effector T cells from the host toward the cancer cells, inducing the latter's lysis by delivery of perforin and granzyme.

The scaffold of blinatumomab is composed of two single-chain variable fragments (scFv) fused with a Gly-Gly-Gly-Gly-Ser (G<sub>4</sub>S) linker. This engineering scheme has been used to design others bispecific agents called bispecific T-cell engagers (BiTE), maintaining their ability to recruit and activate T cells and changing the tumor cells targeting scFv (6). BiTEs are characterized by a conformation that creates an efficient immunologic synapse between T cell and targeted cell. Their relatively small molecular weight of 55 kDa could also provide improved tumor penetration (7), but is associated with a short plasma half-life of approximately 2 hours. Therefore, patients with acute lymphoblastic leukemia (ALL) require an infusion pump to deliver a constant flow rate of blinatumomab (8). Nevertheless, the use of this device is not optimal for patient comfort and contributes to the high cost of the treatment. The replacement of this device by a low-cost long acting biodegradable technology could provide a substantial benefit for patient comfort as well as reduce healthcare costs, and make the treatment approach more available in areas of the world that are resource constrained.

The quest for an appropriate controlled release system for protein therapeutics is challenging, given the intrinsic fragility of the macromolecule as well as the costs of the drug product manufacturing and possibly the device. Over the last decades, intense investigations have been performed using biodegradable and biocompatible polymers as solid implants, particles, or injectable depots to entrap proteins and release them through the degradation of the polymer depot (9–12). The use of a polymeric controlled release system for BiTE-like proteins is an interesting novel approach, but has to fulfill

<sup>1</sup>Department of Urology, Weill Cornell Medical College–New York Presbyterian Hospital, New York, New York. <sup>2</sup>Medincell SA, Jacou, France.

**Note:** Supplementary data for this article are available at Molecular Cancer Therapeutics Online (<http://mct.aacrjournals.org/>).

**Corresponding Author:** Wilhem Leconet, Department of Urology, Weill Cornell Medicine, 525 East 68th Street, F903, New York, NY 10065. Phone: 212-746-5493; Fax: 212-746-8941; E-mail: wil2011@med.cornell.edu

doi: 10.1158/1535-7163.MCT-17-1138

©2018 American Association for Cancer Research.

Leconet et al.

several criteria to preserve the protein integrity, maintain a therapeutic concentration, and avoid any toxicity due to T-cell-related cytokine release risk in case of uncontrolled protein delivery (13). *In situ* forming depots generated by injection of drug/polymer/solvent formulations are an attractive system as the polymeric depot entrapping the active compound could protect the protein and release it in a controlled manner through the erosion and degradation of the polymeric depot (14–17). Parameters such as polymer composition, nature of the solvent, and the state of the protein (solid or in solution) allow to finely tune the final characteristics of the formulation such as its viscosity and the degradation and release kinetics from the depot upon administration (18, 19).

In this study, the scFv of the anti-prostate specific membrane antigen (PSMA) J591 antibody (20) was used to design a BiTE antibody, designated Bij591, targeting PSMA and CD3. After demonstrating the specific cytotoxicity of Bij591 to PSMA-positive prostate cancer models *in vitro* and *in vivo*, the protein was formulated in a long-acting injectable technology drug-delivery system composed of diblock (DB) and triblock (TB) biodegradable polyethylene glycol (PEG)–poly(lactic acid; PLA) copolymers solubilized in tripropionin, a small-chain triglyceride. The stability and functionality of Bij591 throughout the formulation process were demonstrated, and a single dose of a Bij591 polymeric formulation injected subcutaneously significantly improved the apparent elimination half-life as well as the *in vivo* antitumor activity of the bispecific antibody in cancer xenograft models in comparison with a daily intravenous administration.

## Material and Methods

### Expression, production, and purification of Bij591

Bij591 cDNA sequence was synthesized *in silico*, using the GeneArt Gene Synthesis software (Invitrogen), by fusing the VH/VL regions of deimmunized anti-PSMA antibody J591 to the VH/VL region of anti-CD3 antibody OKT-3, using a (G<sub>4</sub>S) linker. 6xHis and c-Myc tags were added at the C-terminal region of the cDNA sequence to purify and detect the recombinant protein (Fig. 1A). Chinese Hamster Ovary (CHO) cells were transfected with the pcDNA3.1-Bij591 plasmid using FreeStyle MAX Reagent according to the manufacturer's protocol (Invitrogen). Bij591 was purified from CHO supernatant using a Cobalt HiTrap TALON column (GE Healthcare), a yield of 10 mg of Bij591 per liter of supernatant was obtained. Analysis of Bij591 purity was performed by SDS-PAGE and Coomassie Blue staining.

### Cell lines and culture

The LNCaP, PC-3 Wild-Type (PC-3 WT), MDA PCa 2b prostate cancer cell lines were obtained from ATCC. CWR22Rv1 and PC3-PSMA were gifts, respectively, from Thomas Pretlow, MD (Case Western Reserve University, Cleveland, OH) and Michel Sadelain, PhD (Memorial Sloan Kettering Cancer Center, New York, NY). PC-3 WT, CWR22Rv1, LNCaP cells were routinely maintained in RPMI1640 (Mediatech, Inc.) supplemented with 10% FBS, 1% penicillin–streptomycin, and 2 mmol/L L-glutamine (all reagents from Gemini Bio-products). MDA PCa 2b cells were grown in F12K medium (ATCC) containing 20% FBS, 1% penicillin–streptomycin, 2 mmol/L L-glutamine, 10 ng/mL EGF (BD Biosciences), 25 ng/mL cholera toxin, 5 μmol/L phosphoethanolamine, 100 pg/mL hydrocortisone, 45 nmol/L selenious acid, and

5 μg/mL insulin (all from Sigma-Aldrich). All cell lines were tested for *Mycoplasma* contamination and authenticated by DNA Diagnostics Center prior to experiments.

### Bij591-dependent cell cytotoxicity and cytokine release

J591 constructs (huJ591, scFvJ591, and Bij591) were incubated at various concentrations with either PBMCs or purified CD3 T cells for 30 minutes. Then, target prostate cancer cells were added at different E:T ratios for 5 hours. Cytotoxicity was measured by lactate dehydrogenase (LDH) release assay using Cytotoxicity Detection KitPLUS from Roche and following the kit's instructions. Human peripheral blood mononuclear cells (huPBMC) were isolated by Ficoll density gradient centrifugation, and enrichment for CD3 T cells was conducted by using RosetteSep Human T-cell Enrichment Cocktail (StemCell Technologies). Cytokines (IL2, IL4, IL6, IL10, IFNγ, and TNFα) release concentration was determined in supernatants of cytotoxicity assays using a commercially available FACS-based cytometric bead array (CBA-Kit, BD Biosciences) in accordance to the manufacturer's protocol.

### PSMA- and CD3-binding studies

The ability of purified Bij591 to bind with both PSMA and CD3 before and after the spray-drying process described below was measured by flow cytometry, using full antibodies J591 and OKT-3 as positive controls and 6xHis-Tag mouse mAb and anti-mouse IgG-alex fluor 488 as secondary antibodies (Thermo Fisher Scientific). To assess Bij591 functionality during the *in vitro* release (IVR) experiment described below, Jurkat and LNCaP cells were incubated with each IVR sample and the Bij591 amount was determined by comparing the fluorescence intensity with a Bij591 standard binding curve performed on both cell lines. For quantitative determination of PSMA cell surface receptors, 1 × 10<sup>6</sup> of each PCa cells/sample were stained with anti-PSMA murine J591 antibody by indirect immunofluorescence using the QIFIKIT (Agilent). PSMA-positive PCa cells (CWR22Rv1, LNCaP, and MDA PCa 2b), setup beads, and calibration beads were given goat anti-mouse IgG-FITC, followed by two washes in PBS-BSA (0.1%) and analysis by flow cytometry on an Accuri C6 flow cytometer (BD Biosciences). The numbers of receptors per cell lines were calculated against fluorescent calibrating bead standards using linear regression.

### Spray drying of Bij591 and particle analysis

Several excipients were added to the protein aqueous solution to maintain its stability (Supplementary Table S1). Bij591 solution was spray dried using a Büchi B290 spray dryer. Inlet temperature, atomization pressure, and liquid feed rate were set at 85°C, 3 bar, and 2 mL/minute, respectively. The outlet temperature recorded during the process was 50°C. Powder was collected and vacuum dried at 25°C under continuous vacuum for 6 hours. The residual moisture content of the spray dried powder was determined by the measurement of weight loss on drying after incubation in a vacuum oven at 80°C for 6 hours. Particle size analysis was performed on the dry powder using a SympaTec HELOS particle size analyzer. Total protein content was determined using a Lowry assay.

### Bij591 formulations preparation

The protein was formulated using MedinCell's proprietary long-acting injectable technology, trademarked as BEPO (21).

This technology is based on a solution of biodegradable DB PEG-PLA and TB PLA-PEG-PLA copolymers dissolved in a bio-compatible solvent, which was tripropionin (Sigma-Aldrich) in this study. To prepare the polymeric vehicle solutions, DB and TB copolymers, provided by MedinCell, were added to tripropionin in a 10 mL glass vial and placed on a roller mixer at room temperature until complete dissolution of the polymer, confirmed by visual inspection. Subsequently, spray-dried Bij591 drug was weighed and dispersed into the polymer vehicles to yield a 6% (w/w) spray-dried cake loading. Final formulations were magnetically stirred until achieving full homogeneity. Different formulations were tested by keeping constant the copolymers: tripropionin: Bij591 weight ratio and changing the composition of the DB. Copolymers used for polymeric candidates are summarized in Supplementary Table S2.

#### Mechanical properties of polymeric vehicles

The dynamic viscosity of vehicles was measured using an Anton Paar MCR301 rheometer. After preparation, vehicles were homogeneously conditioned at 25°C using a Peltier microplate set on the rheometer. A total of 200  $\mu$ L of vehicle was put at the center of the measuring plate. Thereafter, the geometry, a Cone-Plate geometry with a diameter of 25 mm and a contact angle of 2° (CP-25), was lowered, applying a gap of 0.051 mm between the geometry and the measuring plate. A decreasing rotation shear rate from 1,000 to 0.1/second was applied. For each formulation, the mean value ( $n = 3$ ) of the dynamic viscosity at the highest shear rate (1,000/second) was reported in mPa.s. Injectability studies were performed using a texturometer (Lloyd Instruments) in compression mode at room temperature. Polymeric vehicles were loaded in a 0.5-mL syringe equipped with a 23 G, 1-inch needle. The injection force necessary to maintain a constant flow rate of 1 mL/minute was determined in triplicate for each vehicle.

#### IVR and stability of formulated Bij591

IVRs of Bij591 from formulation candidates were performed in a sodium phosphate buffer (pH 6.8) supplemented with 0.005% Tween 80 to avoid protein adsorption at low concentrations. A total of 50  $\mu$ L of each formulation was injected into 20 mL of buffer in glass vials that were capped and placed at 37°C under continuous orbital shaking during 66 days. At given time points, the medium was collected and replaced by preheated buffer. Released protein concentration in the medium was determined by size exclusion (SEC) HPLC analysis. To improve sensitivity, protein quantification relied on the intrinsic fluorescence of the protein (excitation and emission wavelengths were 275 nm and 330 nm, respectively). Cumulative release profiles were built taking into account the total protein cargo contained in the injected formulations. Stability of Bij591 was monitored during 4 weeks in the TB1/DB4 formulation stored at 4°C or room temperature. At each time point, a small amount of formulation (in triplicate) was precisely weighed in a microtube and dissolved in ethyl acetate. After centrifugation, the protein pellet was washed twice with 500  $\mu$ L ethyl acetate and dried for 1 hour in a vacuum oven. Dry pellet was solubilized in 1 mL of release buffer. After centrifugation for 10 minutes at 16,000  $\times g$ , the protein contained in the supernatant was analyzed and quantified by SEC-HPLC.

#### In vivo studies

Mice were purchased from Charles River Labs and all animal procedures were approved by the Institutional Animal Care and Use Committee of Weill Cornell Medicine.

#### Pharmacokinetics of Bij591 solution and formulations

Two *In vivo* pharmacokinetic single-dose studies were carried out in male BALB/c mice weighing 20–30 g that were randomly divided into 3 animals per treatment group. The intravenous Bij591 solution tested in the first pharmacokinetic study at 1 mg/kg allowed to select the dose level to be used in the second study. Subsequently, mice were administered (using a 25G needle) at 15 mg/kg dose level with either subcutaneous Bij591, formulation TB1/DB1 or TB1/DB4 (selected on the basis of the IVR data), or subcutaneous (interscapular area), or intravenous Bij591 solution. The volume injected was 50  $\mu$ L (ca. 2.5 mL/kg) of formulation or PBS pH 7.4 solution. Blood samples (100  $\mu$ L) were collected from Bij591-treated animals only at the following time points (3 animals per time point): 0 (predose), 1, 3, and 7 hours, and then 1, 2, 4, 7, 9, 11, 14, 16, and 21 days after administration.

Bij591 plasma concentrations were determined by the following ELISA assay: Anti-PSMA 7E11 (40  $\mu$ g/mL), binding a cytosolic epitope of PSMA, was coated to High Bind Microplates (Costar) plate and incubated overnight at 37°C. LNCaP membrane preparation was then added to each well. After 2-hour incubation at room temperature and 3 wash cycles with PBS-Tween (0.05%), Bij591 standards, controls, and mouse plasma samples were added and incubated for 4 hours at room temperature. After another PBS-T wash step, Bij591 was targeted adding a rabbit anti-6His epitope tag antibody (1:1500, Genscript) for 1 hour at room temperature. The plates were then washed with PBS-T and an alkaline phosphatase-conjugated anti-rabbit IgG secondary antibody diluted 1:5,000 was added and incubated in each well for 1 hour at room temperature. After a last PBS-T wash, 100  $\mu$ L of PNPP substrate (Thermo Fisher Scientific) was added to each well. After 30 minutes, the optical density was measured at 405 nm using a plate reader. Bij591 concentration in each plasma sample was determined according to the standard optical density measured at the same time.

Individual pharmacokinetic parameters such as  $C_0$  (intravenous),  $C_{max}$ , and  $t_{max}$ ,  $C_{last}$ , and  $t_{last}$ , area under the curve (AUC), and half-life ( $t_{1/2}$ ) were then calculated using the validated software Phoenix 64 WinNonlin Version 7.0 (Pharsight Corporation). The plasma concentration–time data obtained for each formulation were analyzed using a noncompartmental analysis (NCA) for both routes (intravenous and subcutaneous). The absolute subcutaneous bioavailability was estimated on the basis of the intravenous and subcutaneous AUCs extrapolated to infinity.

#### Paraffin embedding and histologic assays

The polymeric depots, tissues, and tumors of all mice were formalin fixed, embedded in paraffin blocks, and sectioned (5  $\mu$ m). For immunogenicity assays, sections were stained with hematoxylin and eosin (H&E) and provided to a pathologist who examined the degree of inflammation of the tissue surrounding the polymeric depot. To observe T-cell infiltration, tumor and injection site skin sections were processed for immunostaining using anti-human CD3 antibody (Dako) and appropriate

Leconet et al.

peroxidase-conjugated secondary antibody (Jackson Immuno-Research). Histologic images were taken by using a CX41 microscope and an OMAX A3550U digital camera (Olympus).

#### Hematologic assays

A group of 15 BALB/c mice was administered subcutaneous with 50  $\mu$ L of the vehicle of TB1/DB4 formulation, that is, a polymeric solution with similar copolymers concentration to that of the formulation, without Bij591. Another control group of 15 BALB/c mice was injected subcutaneous a similar volume of PBS. The amount of circulating white blood cell (WBC), neutrophil (NEU), monocyte (MON), lymphocyte (LYM), red blood cell (RBC), hemoglobin (HGB), platelet (PLT), and the mean platelet volume (MPV) were recorded after each blood withdrawal (50–100  $\mu$ L at days 1, 7, 14, 21, and 28) using a complete blood count (CBC) instrument.

#### Bij591 formulation antitumor activity

LNCAp ( $10 \times 10^6$ ), CWR22Rv1, PC-3 WT, or PC-3 PSMA cells ( $5 \times 10^6$ ) were injected subcutaneously (flank area) with Matrigel (Corning) in 6–8 week-old male SCID mice. When tumors reached a minimum volume of 150–200  $\text{mm}^3$ , tumor-bearing mice were randomized in different treatment groups ( $n = 8$  per group) and were treated with a single intravenous injection of huPBMCs ( $5 \times 10^6$ ). Two hours later, mice were administered either a single subcutaneous injection (interscapular area) of Bij591 TB1/DB4 formulation (15 mg/kg in 50  $\mu$ L), or a single subcutaneous injection of Bij591 solution (15 mg/kg in 50  $\mu$ L), or a daily intravenous injection of Bij591 solution (1 mg/kg in 200  $\mu$ L daily for 15 days), or a daily intravenous injection of huJ591 solution (1.5 mg/kg in 200  $\mu$ L per day during 15 days). The control mice groups were administered either 50  $\mu$ L s.c. TB1/DB4 polymeric vehicle (interscapular region) or a daily intravenous injection of PBS (200  $\mu$ L per day during 15 days). Tumors were measured using a caliper and volume was calculated using the formula  $V = (\text{tumor length} \times \text{tumor width} \times \text{tumor depth})/2$ . Concerning the PC-3 WT/PC-3 PSMA xenografts growth study, explanted tumors were photographed and weighed at the end of the experiment.

#### Statistical analysis

The level of significant difference in tumor volume progression was determined by the two-way ANOVA. All statistical analyses were performed using Prism Version 5 (GraphPad Software). A  $P$  value of less than or equal to 0.05 was considered significant in all analyses herein. Descriptive statistics of the pharmacokinetic parameters were performed.

## Results

#### Purification and characterization of the recombinant PSMA/CD3 Bij591

After large-scale production in CHO cells and purification, analysis by SDS-PAGE gel showed a 55-kDa protein corresponding to the expected size of the bispecific antibody (Fig. 1B) with a similar purity (95%–98%) and yield than the scFv of J591 antibody (10 mg per liter of CHO supernatant). By flow cytometry, Bij591 binding to PSMA and CD3 was compared with the two parental mAbs used to design this bispecific antibody, HuJ591, which is a deimmunized version of anti-PSMA J591 antibody (20, 22), and OKT-3, a murine mAb targeting CD3

(23). Bij591 was shown to bind to PSMA-positive LNCAp PCa cell line and CD3-positive Jurkat T cells, keeping the binding properties of the parental mAbs with an apparent lower affinity to CD3, which could be explained by the proximity of the 6 $\times$ His-Tag used to detect the Bij591 and binding site to CD3 (Fig. 1C). SEC-HPLC analysis of the purified Bij591 showed a major peak and two larger species of the bispecific, probably dimer and trimer or multimer (Supplementary Fig. S1A). Each peak was purified and showed similar binding properties to PSMA and CD3 (Supplementary Fig. S1B and S1C). Finally, no binding signal was detected with PSMA/CD3-negative PC-3 WT PCa cells (Supplementary Fig. S2A).

#### Bij591 mediates T-cell activation and cytotoxicity of PSMA-positive PCa cell lines

The potency of Bij591 to induce T-cell cytokine release in the presence or absence of PSMA-positive LNCAp cells after 24 hours of incubation was first assessed by flow cytometry. A Bij591 dose-dependent increase of the 6 different cytokines was observed only when LNCAp and T cells were coincubated with the bispecific antibody (Fig. 2A). In the absence of LNCAp cells, there was no substantial variation in the cytokine release profile of T cells. Upon Bij591 incubation, IL2, an interleukin that promotes the proliferation and differentiation of T cells into effector and memory T cells (24), was the most increased cytokine in these experiments (~240-fold).

Next, we compared the capacity of Bij591, humanized J591 (huJ591) and the scFv J591, as a negative control, with redirect purified human PBMCs and T-cell lysis against PSMA-negative (PC-3 WT), PSMA-low (CWR22Rv1) and PSMA-high (LNCAp, MDA PCa 2b) prostate cancer cell lines (Supplementary Fig. S2A and S2B). Although no lysis was observed when the three J591 constructs were coincubated with PC-3 WT and huPBMCs/T cells, we showed that Bij591-mediated killing was higher than the antibody-dependent cell cytotoxicity induced by huJ591 on PSMA-positive PCa cells and its  $EC_{50}$  was positively correlated with the surface expression of PSMA in these cell lines (Fig. 2B). Moreover, Bij591 was the only construct able to induce PSMA-positive PCa cells lysis by purified T cells (Fig. 2C). Finally, the cytotoxic efficiency of Bij591 was analyzed and compared with the molar equivalent concentration of huJ591 at different E:T ratios in LNCAp cells. As shown in Fig. 2D, Bij591 provides more efficient huPBMCs and T-cell cytotoxicity than huJ591. Thus, these results demonstrate that Bij591 is able to induce a PSMA-specific dose-dependent activation and T-cell-mediated killing of PCa cells.

#### Bij591 displays short half-life and strong antitumor activity in mouse models

To determine how frequently Bij591 should be administered for tumor therapy *in vivo*, the preliminary pharmacokinetic analysis of the bispecific antibody was performed in BALB/c mice. After intravenous injection of 1 mg/kg Bij591, the plasma Bij591 concentration was measured by ELISA, demonstrating a half-life of approximately 9 hours (Fig. 3A). On the basis of these results, a daily treatment of 1 mg/kg for 15 days was applied in our xenografts models. Then, the antitumor efficacy was evaluated after a daily treatment of NOD-SCID mice harboring established LNCAp xenografts with Bij591 intravenously for 2 weeks (1 mg/kg/day) compared with PBS-treated and huJ591-treated (1.5 mg/kg/day, the molar equivalent of the

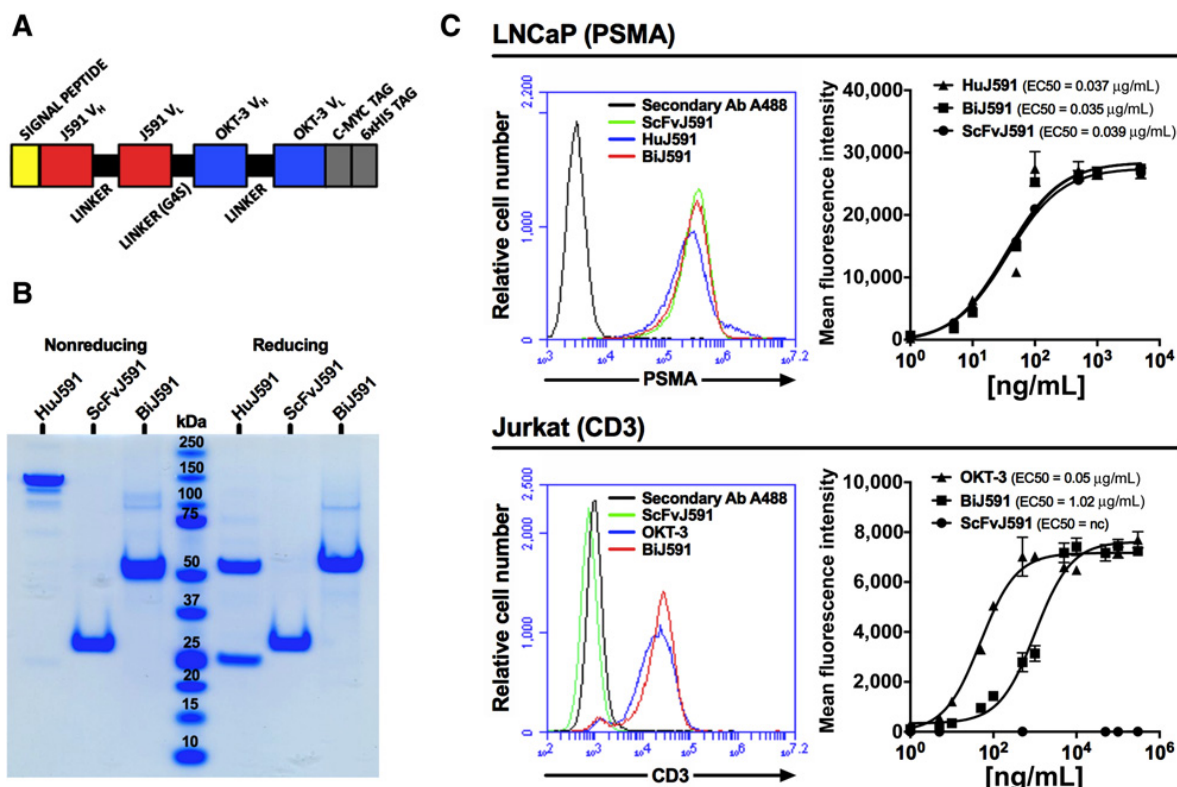


**Figure 1.**

Design, purification, and characterization of the recombinant human PSMA/CD3 BiJ591. **A**, Schematic representation of BiJ591. **B**, Purity and molecular weight analysis of BiJ591 compared with huJ591 and scFvJ591 by SDS-PAGE (4  $\mu$ g protein per well in nonreducing and dithiothreitol 5 mmol/L reducing conditions) and Coomassie Blue staining. **C**, Binding of BiJ591, scFvJ591, huJ591, and OKT-3 to human PSMA and CD3 receptors by flow cytometry. LNCaP (PSMA<sup>+</sup>) and Jurkat (CD3<sup>+</sup>) cells were incubated with various concentrations (0.001–300  $\mu$ g/mL) of antibodies and stained with a fluorescent secondary antibody.

BiJ591 dose) animals. A significant growth inhibition of the BiJ591 group was observed compared with saline and huJ591-treated animals ( $P < 0.0001$  for both). Specifically, the mean tumor volume in BiJ591-treated mice was reduced by 57% at day 33 compared with 16% for the huJ591-treated mice (Fig. 3B). Moreover, the T-cell infiltration into the tumor during the treatment in BiJ591 and control groups was analyzed by IHC. Whereas T cells were detected in the tumor stroma of control group tumors up to 1 week, a daily treatment with BiJ591 resulted in T cells within the stroma for 2 weeks as well as infiltrating the center of the tumor (Fig. 3C).

#### Characterization of spray-dried BiJ591

To preserve the functionality and integrity of the bispecific antibody within the polymeric formulation, choice was made to maintain it in its solid-state form throughout the formulation process. After spray drying the protein, a monodispersed particle size distribution was obtained (Fig. 4A). Particle size was measured by laser diffraction and mean volume diameter was determined to be 9.66  $\mu$ m. Final water content in the as-obtained powder was determined as 3.1% (w/w). Particle size values  $d_{10}$ ,  $d_{50}$ , and  $d_{90}$  were, respectively, 2.88, 7.31, and 19.71  $\mu$ m. The protein content in the spray-dried cake was confirmed to be 10%

(w/w). Then, using flow cytometry, BiJ591 was shown to preserve its binding properties to PSMA and CD3 before and after spray drying. (Fig. 4B).

#### Polymeric formulations preserve BiJ591 stability and control its release *in vitro*

The rheological and injectability behavior of the BiJ591 polymeric vehicles are shown in Fig. 4C. These formulations differ only by the PLA:PEG ratio of the DB (Supplementary Table S2), whose value is correlated to the hydrophobicity of the formulation, and show an increase of both viscosity and injectability directly related to this ratio. The obtained values of viscosity and injectability of these vehicles are within the acceptable specifications determined by the provider for the production scalability and a clinical utilization, reinforcing the potential of these drug products. Once the physicochemical characteristics of the selected vehicles were demonstrated to be acceptable, these vehicles were used to formulate BiJ591. Figure 4D shows the *in vitro* dissolution profile of the bispecific antibody from each of these formulations. The release profile of BiJ591 from TB1/DB1 shows a fast-initial release phase of 50% of the bispecific antibody during the two first weeks and a slower second phase. Concerning the three other formulations,

Leconet et al.

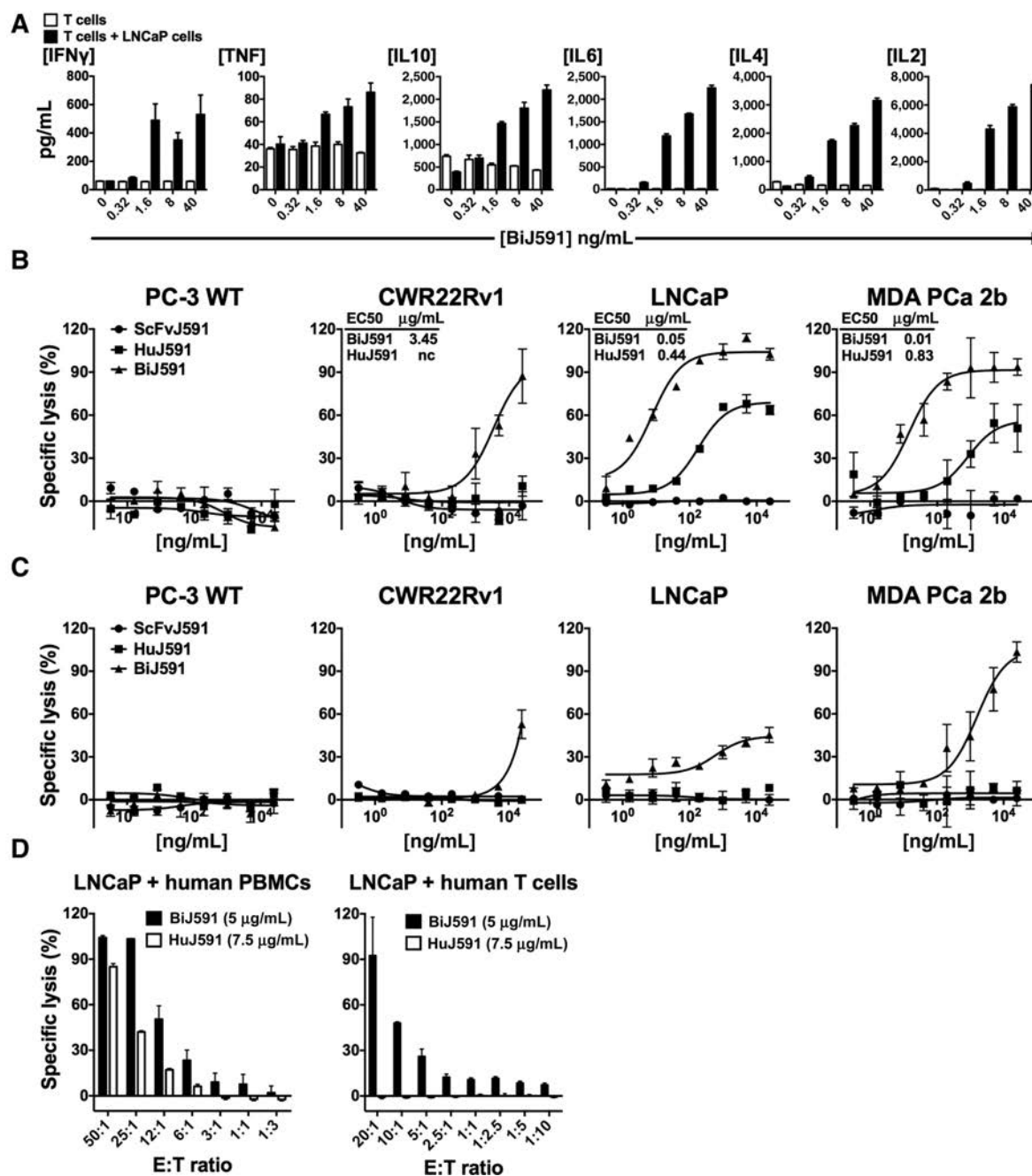


Figure 2.

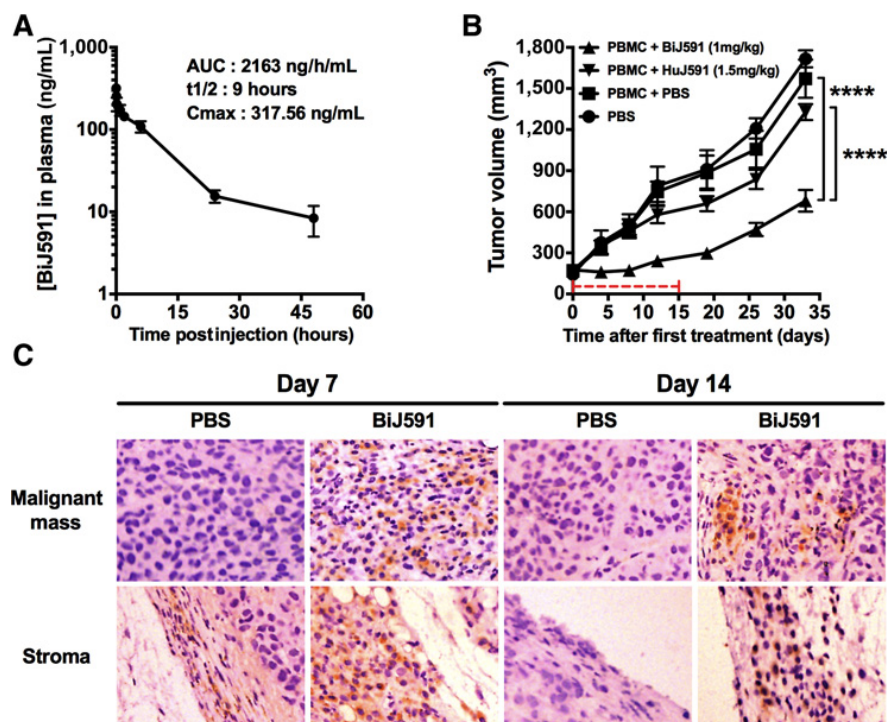
*In vitro*-specific cytotoxicity of BiJ591 to PSMA-positive prostate cancer cell lines. **A**, Cytokine release of purified T cell in presence or not of LNCaP cells and increasing concentrations of BiJ591. Cytokine concentration was determined by cytometry-based bead assay. **B–D**, BiJ591-dependent cell lysis on PCa cell lines coincubated with human PBMCs (whole WBC population, including lymphocytes and monocytes) or purified T cells. After 5 hours of coincubation at 37°C, specific lysis was compared with scFvJ591 and huJ591 at several concentrations (**B** and **C**) and E:T ratios (**D**) and was determined dosing the lactate dehydrogenase (LDH) released by lysed prostate cancer cells lines (nc, not calculable).

a lower initial burst and a lag phase were observed before a subsequent slower release step. Surprisingly, the relationship between the release profile and the enhancement of the vehicle

hydrophobicity and viscosity was not clear. It was expected that formulations containing hydrophilic copolymers would yield more porous depots where the diffusion of the bispecific

**Figure 3.**

Pharmacokinetics and antitumor activity of Bij591. **A**, Pharmacokinetics of Bij591 was conducted in BALB/c mice after intravenous injection of 1 mg/kg bispecific antibody and measuring its plasma concentration by ELISA assay. **B**, Effect of Bij591 on subcutaneous LNCaP xenograft growth in NOD/SCID mice ( $n = 6$  mice per group). A total of  $1 \times 10^7$  LNCaP cells were injected subcutaneously in the right flank of NOD/SCID mice. When tumors reached approximately  $150 \text{ mm}^3$ , 3 groups were injected intravenously with human PBMCs. Two hours later, mice were treated daily with 1 mg/kg of either huJ591 or Bij591, or saline for 2 weeks (red dotted line). Results are presented as the mean tumor volume  $\pm$  SEM for each group; \*\*\*\*,  $P < 0.0001$ . **C**, Histologic detection of human T-cell infiltration in LNCaP tumors during Bij591 treatment. Staining for human CD3<sup>+</sup> T cell was detected by IHC and displayed at a 50 $\times$  magnification.



antibody to the aqueous medium would be enhanced. Indeed, the fastest release was observed with the less hydrophobic formulation TB1/DB1. However, there were no substantial differences among the three other formulations despite the different hydrophobicity of the polymers within the formulation. In parallel to the IVR, the amount of released Bij591, from TB1/DB1 and TB1/DB4, able to bind PSMA and CD3 was also measured. The release profile of functional Bij591 obtained from these flow cytometry studies on LNCaP and Jurkat cells was similar to the SEC-HPLC profile demonstrating that the bispecific antibody integrity was preserved within the depots throughout the IVR duration (Fig. 4E). Moreover, stability of Bij591 in the TB1/DB4 formulation was investigated at 4°C and room temperature storage conditions (Fig. 4F). A protein recovery between 94% and 99% at both temperatures during the first 3 weeks was observed while a slow decrease (92%) at day 28 could be noted. Altogether, these results confirm that the polymer-based technology can control the delivery of the protein, although preserving its functionality in the formulation as well as in the solid depot. Regarding these results, the ability of the formulations with the most disparate viscosity/hydrophobicity properties (TB1/DB1 and TB1/DB4) to control the release of the bispecific antibody was evaluated *in vivo*.

#### Polymeric formulations improve substantially Bij591 stability and pharmacokinetic parameters

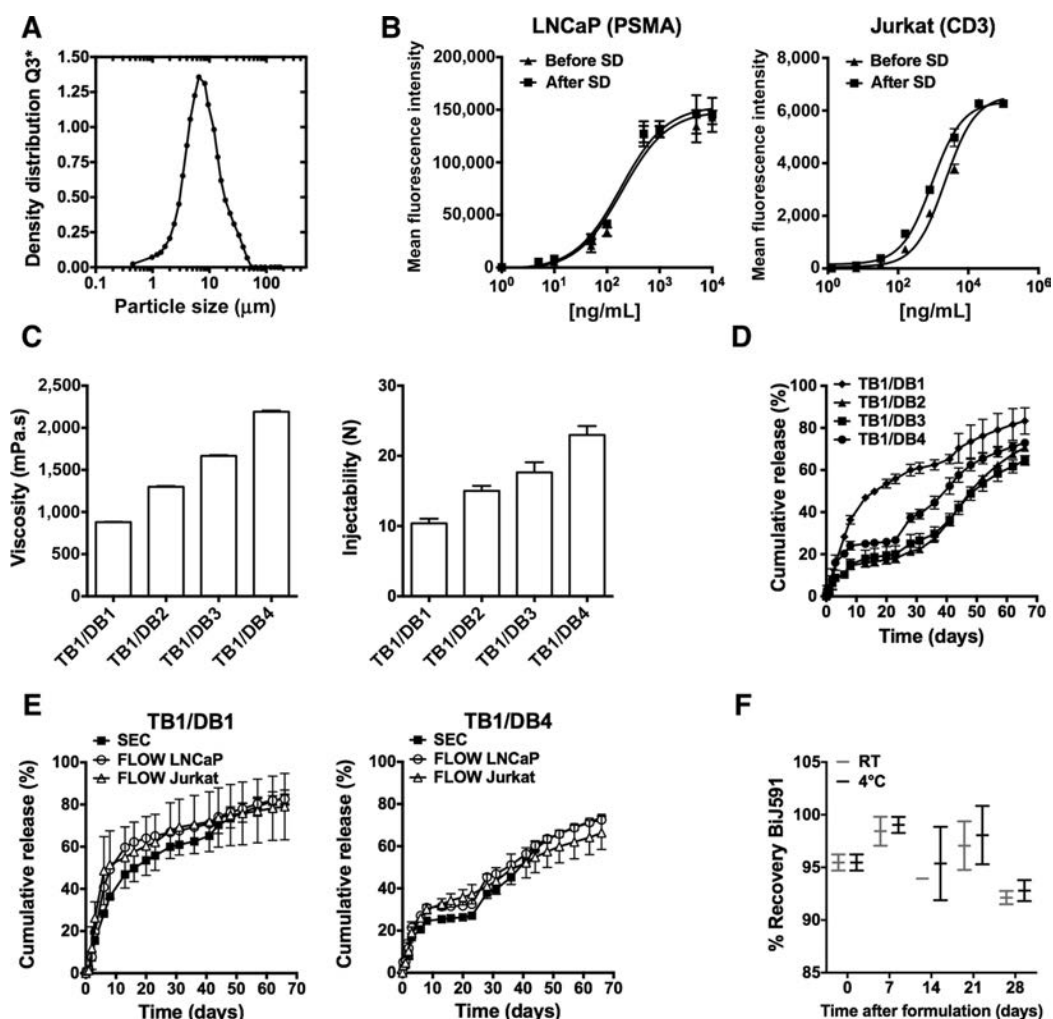
Following the results obtained during the first *in vivo* antitumor assay, a 15 mg/kg dose level of Bij591 has been selected to be equivalent to a 2 weeks daily treatment at 1 mg/kg. The semilogarithmic plot of the mean plasma concentration–time curves of Bij591 formulation candidates TB1/DB1 and TB1/DB4 after subcutaneous dose was compared with those

of unformulated Bij591 after intravenous and subcutaneous dose as shown in Fig. 5A. The plasma concentrations and the main pharmacokinetic parameters are reported in Supplementary Tables S3 and S4, respectively. The expected pharmacokinetic outcomes were reached as these candidates positively modified the pharmacokinetic profile of the protein; the maximum plasma levels ( $C_{max}$ ) were, respectively, 11- and 1.5-fold lower than the bolus intravenous and subcutaneous injections, whereas the half-life of the bispecific antibody was improved from 16 hours to up to 4 days and 8 days for TB1/DB1 and TB1/DB4, respectively. In addition, the AUC and the bioavailability of the protein released from the formulation candidates was increased up to 1.9-fold compared with the subcutaneous bolus of Bij591 solution (same injection site for the three subcutaneous formulations). Moreover, both candidates provided a sustained release of the protein over time, with plasma concentrations still quantifiable after 21 days postadministration. However, the most hydrophobic and viscous formulation, TB1/DB4 candidate, provided the highest sustained plasma levels from day 9 onwards. Encouragingly, these results correlate with the delivery profiles obtained *in vitro* as the release from TB1/DB4 formulation was the slowest one in both experiments. On the basis of this long-term release *in vivo*, the TB1/DB4 formulation candidate was selected for the following studies.

#### TB1/DB4 polymeric vehicle showed no blood toxicity and low inflammation *in vivo*

Possible hematologic toxicity and inflammation of the TB1/DB4 vehicle were evaluated over a month after subcutaneous injection in BALB/c mice by complete blood count (CBC) and IHC of the injection site. As shown in Fig. 5B and

Leconet et al.

**Figure 4.**

*In vitro* characterization, functionality, and release of BiJ591 formulated in polymeric vehicles. **A**, Particle size distribution of spray-dried BiJ591 determined by laser diffraction. **B**, Binding of various concentrations (0.001–100 μg/mL) of BiJ591 before and after spray drying to PSMA and CD3 receptors by flow cytometry. **C**, Effect of the molecular ratio of PLA units over PEG units in polymeric vehicles DB on their viscosity and injectability. **D**, Impact of the PLA:PEG DB ratio on BiJ591 *in vitro* release from polymeric formulations. All formulations contained 6% of spray-dried BiJ591. The protein was dosed by SEC-HPLC. **E**, Analysis of the amount of BiJ591 able to bind PSMA and CD3 after IVR from TB1/DB1 and TB1/DB4 formulations by flow cytometry. Each time point PSMA or CD3 binding fluorescence intensity was compared with a standard BiJ591 curve to determine the amount of functional BiJ591 and compare it with the IVR dosing by SEC-HPLC. **F**, Stability of BiJ591 in TB1/DB4 formulation at 4°C and room temperature. Formulation was dissolved in ethyl acetate and BiJ591 was analyzed and quantified by SEC-HPLC.

Supplementary Table S5, white blood cells counts were equivalent to those obtained after subcutaneous administration of PBS, with some variations in the monocyte population (MON) but not exceeding 1.6-fold (day 21). Animal health parameters such as red blood cells (RBC), hemoglobin (HGB), and hematocrit (HCT) were in the same range as the control (Fig. 5B). Although some hematologic parameters appeared lower than the standard BALB/C range, they were similar to the PBS control group at each time point and might be due to the sensitivity of the instrument (Supplementary Table S5). Histologic analysis revealed slight inflammation characterized by an acute reaction occurring during the first week with infiltration of

polymorphonuclear leukocytes (PMN), mostly basophils, around the depot (Fig. 5C). The depot gradually degraded, becoming smaller and multilocular, and the inflammation evolved into subacute histology, with less granular basophil cells, and then chronic (presence of fibroblasts and fibrosis). No antigen-related inflammation (no multinuclear macrophages) was detected.

#### BiJ591 TB1/DB4 formulation improves T-cell infiltration and antitumor activity *in vivo*

Because a correlation between BiJ591 therapeutic effect and CD3 T-cell infiltration was observed (Fig. 3C), we sought to

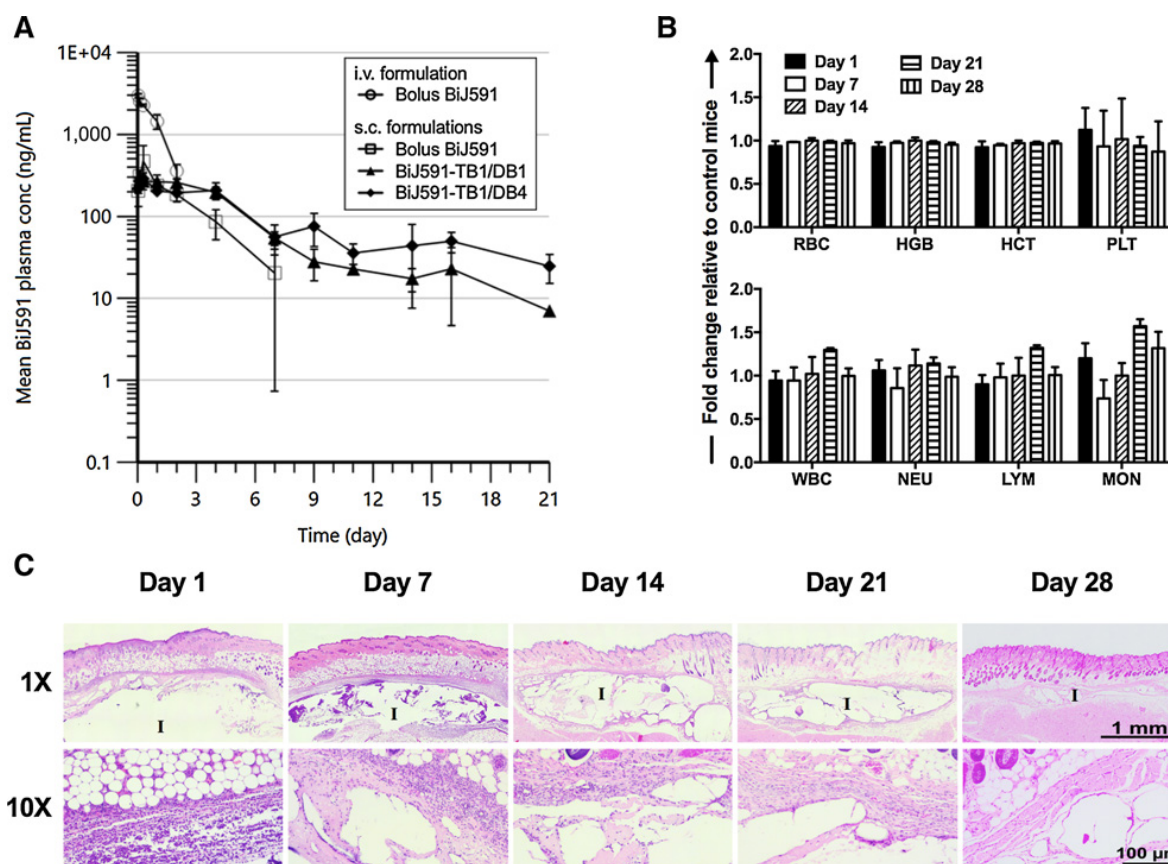


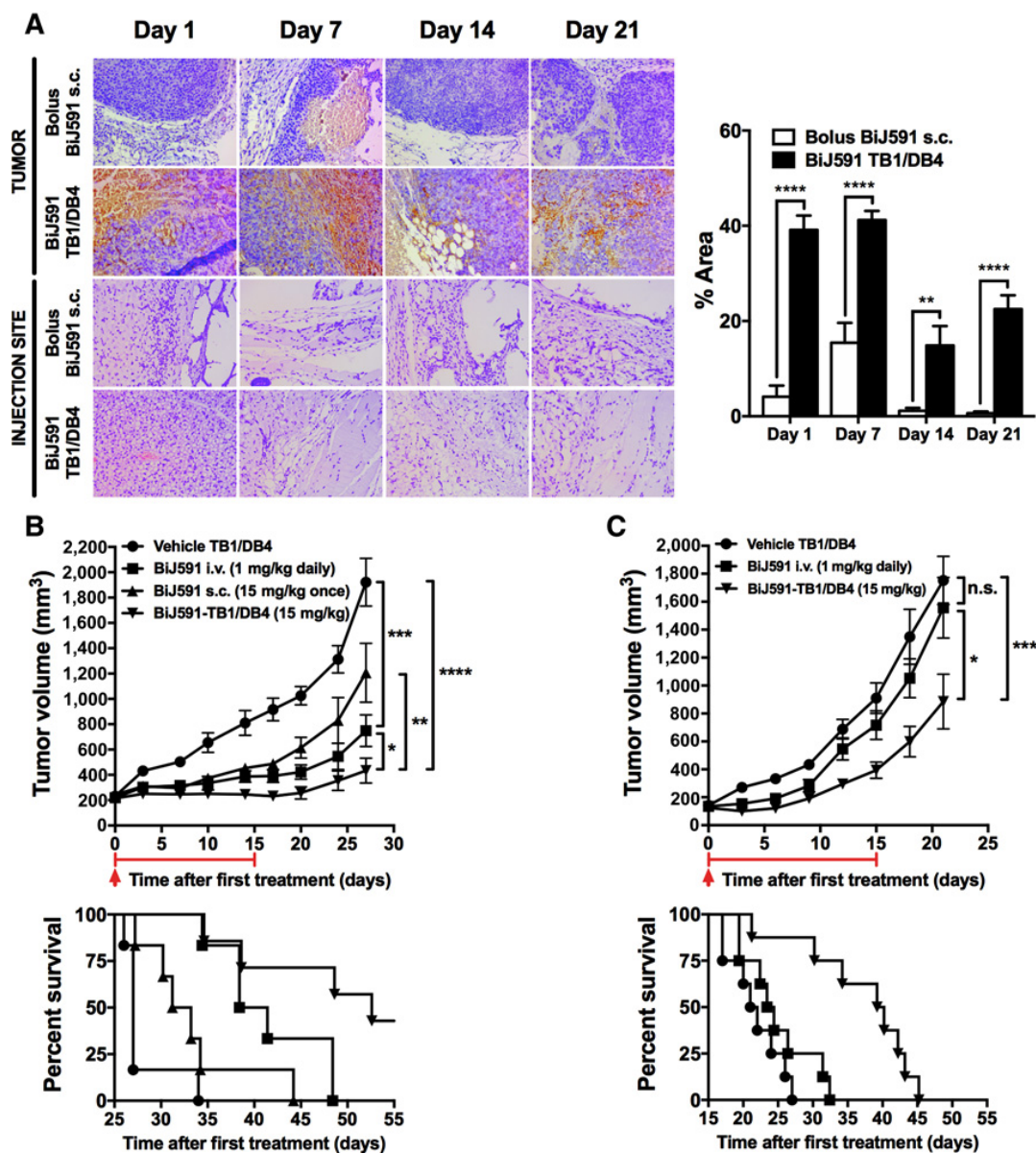
**Figure 5.** Pharmacokinetics and immunogenicity of Bij591-polymeric formulations. **A**, Plasma Bij591 concentration was dosed after either subcutaneous or intravenous administration of 15 mg/kg Bij591 in solution or subcutaneous injection of 15 mg/kg Bij591 formulated in TB1/DB1 or TB1/DB4. Pharmacokinetics parameters were then calculated and summarized in Supplementary Table S4. **B**, CBC after subcutaneous administration of TB1/DB4 vehicle (50 μL) compared with injection of saline. The histograms represent the fold changes of several blood parameters (RBC, red blood cells; HGB, hemoglobin; HCT, hematocrit; PLT, platelets; WBC, white blood cells; NEU, neutrophils; LYM, lymphocytes; and MON, monocytes) relative to the PBS group at 5 time points after administration (days 1, 7, 14, 21, and 28). **C**, Histologic analysis of the injection site after injection of TB1/DB4 vehicle. Sections and H&E staining were performed around the injection site (I = implant) to identify infiltrated immune cells and fibrosis.

dissect the effects of TB1/DB4 on T-cell infiltration of LNCaP tumors compared with a single subcutaneous administration of the same quantity of Bij591 in solution (Fig. 6A). IHC characterization of T cells in LNCaP tumor xenografts of NOD-SCID mice treated with Bij591-TB1/DB4 formulation revealed a substantial infiltration of CD3<sup>+</sup> T-cells for at least 21 days. In contrast, administration of Bij591 subcutaneous in solution had little effect on T-cell infiltration. Concerning the injection site, we did not observe any presence of human T cells in both bolus and polymer groups.

Then, *in vivo* antitumor efficacy of formulated Bij591 was examined in high PSMA LNCaP and low PSMA CWR22Rv1 xenografts (Fig. 6B and C). Drug administration was preceded 2 hours before by intravenous administration of human PBMCs. Compared with the PBS control group, LNCaP tumor growth rate in mice treated with Bij591-polymeric formulation depot was slower and tumor volume was significantly smaller than mice treated with intravenous or subcutaneous Bij591

solution ( $P = 0.0215$  and  $0.0035$ , respectively). Moreover, the median delay to reach a tumor volume of  $2,000 \text{ mm}^3$  was much longer in the Bij591 formulation group (+25 and +14 days vs. control and intravenous bolus Bij591, respectively). Concerning CWR22Rv1 xenografts, a significant antitumor activity ( $P = 0.0005$ ) of the formulated Bij591 was observed compared with the control vehicle group and a daily injection intravenous of Bij591. The median delay to reach a tumor volume of  $2,000 \text{ mm}^3$  was also longer (+18 and +16 days vs. control and intravenous bolus Bij591, respectively). To ensure that the therapeutic effect was specific to PSMA expression, a third *in vivo* experiment was conducted, consisting in injecting PC-3 wild-type subcutaneously and PSMA-transfected cells, respectively, into the left and the right flank of each mouse followed by later treatment with either polymer vehicle, Bij591 daily solution intravenous or Bij591-TB1/DB4 formulation (Fig. 7A). No differences of tumor growth rate between the two cell lines in the polymer vehicle group were measured,

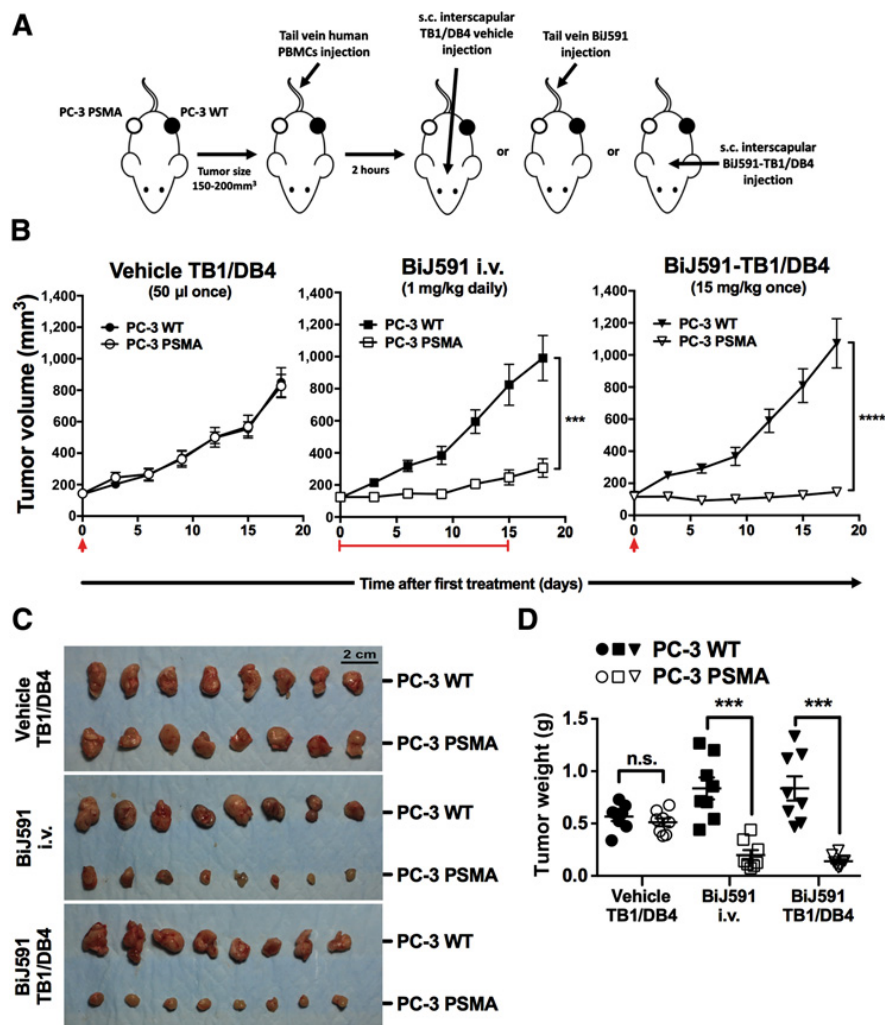
Leconet et al.

**Figure 6.**

*In vivo* therapeutic activity of BiJ591-TB1/DB4 in high- and low-PSMA xenograft models. **A**, Histologic detection of human T-cell infiltration around LNCaP tumors and injection site at 4 time points after subcutaneous administration of either BiJ591 saline solution or BiJ591-TB1/DB4 (magnification, 20 $\times$ ). Tumor T-cell infiltration was then quantified as % positive areas for each experimental group. **B** and **C**, NOD/SCID mice ( $n = 8$  per group) were engrafted subcutaneous in the right flank with either LNCaP or CWR22rv1. When tumor size reached 150–200 mm<sup>3</sup>, all groups received intravenous administration of human PBMCs. Negative control group was inoculated subcutaneous with TB1/DB4 vehicle (single injection, red arrow), whereas the other groups received the indicated doses of BiJ591 in solution either intravenous (2 weeks daily injection, red line) or subcutaneous (single injection, red arrow) or formulated in TB1/DB4 subcutaneous (single injection, red arrow). Tumor size was measured twice a week and modified Kaplan-Meier survival curves represent the percentage of mice with tumor volume < 2,000 mm<sup>3</sup> as a function of time after first treatment. \*,  $P < 0.05$ ; \*\*,  $P < 0.01$ ; \*\*\*,  $P < 0.001$ ; \*\*\*\*,  $P < 0.0001$ .

whereas treatment with BiJ591 intravenous or formulated bi-specific antibody translated into a significant delay of the tumor progression of PC-3 PSMA only (Fig. 7B). These results were confirmed by harvesting and weighing the tumors

(Fig. 7C and D). Altogether, these *in vivo* results demonstrate that the BiJ591 formulation significantly reduces prostate tumor xenograft growth and is even more efficient than a daily administration of the drug for a same therapeutic dosing.



## Discussion

Small antibody fragments have recently emerged as new therapeutic and medical imaging tools in cancer, particularly due to their better tissue penetrance, their capacity to be produced in prokaryotic models and their ability to preserve the binding properties of their parental antibodies (25). Nevertheless, it becomes challenging, like other small proteins, to control and maintain the circulating therapeutic plasma concentrations of these fragments as they are generally rapidly excreted through the kidney. Several strategies for half-life extension have been proposed using genetic fusion or chemical conjugation of the antibody fragment to an IgG Fc, human serum albumin, or polyethylene glycol (26). Some of these strategies have been applied to small bispecific antibody constructs (27–33) with preclinical reported success, but they all imply a modification of the original protein and a plasma exposure of a higher quantity of drug at the beginning of the administration, which could become a disadvantage regarding its potential toxicity. Concerning blinatumomab, infusion of a constant concentration of the drug using a

pump enables to keep the drug level between the therapeutic and toxic range but can become challenging for the comfort and mobility of the patient. In this study, a biocompatible and biodegradable delivery method was designed to sustain the release of a BiTE, BiJ591, in prostate cancer xenograft models and potentially reduce/eliminate tumor burden.

The bispecific antibody was generated by fusing the scFv of J591, a clinical stage deimmunized mAb targeting PSMA, and the scFv of the clinically approved anti-CD3 OKT-3 antibody (20, 22, 23). Like other similar studies testing anti-PSMA/CD3 bispecific antibodies (34–36), the ability of BiJ591 to bind both PSMA and CD3, and also to induce a PSMA-specific cytotoxicity *in vitro* was demonstrated. *In vivo*, the short half-life and the therapeutic effect of this bispecific antibody on PSMA-positive PCa xenografts have been confirmed after daily intravenous injection.

The challenge when changing the method of administration from a daily intravenous treatment to a single subcutaneous long-acting injection is to preserve the stability and the functionality of the protein in the polymeric microenvironment.

Leconet et al.

Furthermore, antibody fragments tend to be unstable and to aggregate rapidly in a soluble state. To overcome this issue, the strategy was first to add stabilizing excipients like trehalose and Tween80, for protecting Bij591 from aggregation and from elevated temperatures induced by the spray-drying process (37, 38). Indeed, spray-dried material was preferable to lyophilized material for obtaining homogeneous dispersion in the polymer vehicles, especially at high API loadings (S. Grizot; unpublished observations). Spray-drying conditions were selected to preserve Bij591 functionality during the process. To control the delivery of the bispecific antibody, an injectable polymeric technology relying on the formation of a depot *in situ* was used. More specifically, the core of the technology allows formulating a drug with a combination of TB and DB PEG-PLA copolymers solubilized in a solvent. Upon contact with aqueous environment, the copolymers precipitate entrapping the drug within the formed depot. The release of the drug occurs when parallel processes of solvent diffusion and degradation of the formed polymeric depot start. The combination of TB and DB PEG-PLA copolymers allows fine tuning the hydrophilic/hydrophobic balance of the formulation, which dictates the release kinetics of the drug as well as the degradation rate of the polymeric matrix. In this particular study, copolymers were dissolved in tripropionin, a carbon C3 small-chain triglyceride similar to triacetin, which has been used in several *in situ* forming gel studies (39, 40), to obtain a viscous injectable solution. While few toxicity studies have been performed with the use of tripropionin (41), some preliminary subcutaneous injection assays were conducted in rats and mice confirming the solvent biocompatibility (S. Grizot; unpublished observations). Tripropionin does not solubilize spray-dried protein molecules, keeping them in their solid-state within the liquid formulation and inside the depot after injection. The mechanical characteristics of the bispecific antibody formulations using 4 different combinations of TBs and DBs were within the acceptable ranges provided by the copolymers provider, MedinCell, and defined on the basis of a product that is currently in clinical development. Very encouragingly, all of them were able to sustain the *in vitro* release of the bispecific antibody for more than 7 weeks. Moreover, the functionality of the released bispecific antibody (from the polymer system) to bind both PSMA and CD3 receptors was maintained. *In vivo*, the subcutaneous polymeric formulations allowed to control and maintain the circulating plasma concentrations over the duration of the study at higher Bij591 plasma levels compared with unformulated Bij591 solutions, administered subcutaneously or intravenously. The  $C_{max}$  after subcutaneous injection of formulated Bij591 was reduced compared with the intravenous route and contributed to a slower decrease of the plasma concentrations of Bij591; indeed, the  $C_{max}/C_{last}$  ratio was in the same order for intravenous solution (ratio of 9) and subcutaneous formulated TB1/DB4 (ratio of 12) but over a different timeframe period, that is, a 2-day period for intravenous route and a 20-day period for subcutaneous route. The sustained release profile observed with the subcutaneous formulated Bij591 significantly impacted the elimination half-life, which was increased and therefore should extend the protein activity. In addition, the formulation was demonstrated to be fully compatible *in vivo*, with an absence of chronic inflammation at the injection site and no change of hematologic parameters up to 1 month after subcutaneous administration.

Macroscopic analysis of the depot and surrounding tissues showed a minor acute inflammatory change related to the injection.

We pursued our *in vivo* studies by evaluating the antitumor activity of the formulated bispecific antibody. Even if the polymeric delivery system was injected distant from the tumor site, the controlled release of the bispecific antibody maintained the presence of human PBMCs within the prostate cancer xenograft for at least 21 days. Regarding the antitumor activity of the delivery system and comparing with a daily administration of Bij591 for 2 weeks, a single subcutaneous injection of TB1/DB4 formulation containing an equivalent total amount of drug showed an improved growth inhibition of prostatic xenografts. This improvement was even more pronounced in low PSMA-expressing tumors like CWR22rv1, where a daily administration of the drug was unable to induce a significant therapeutic effect, whereas the controlled delivery approach did have an impact on tumor growth. This might be explained by the continuous presence of the bispecific antibody in the circulation over a longer duration. Moreover, the antitumor effect was specific to the controlled release of Bij591 and not to the presence of copolymers or solvent as PSMA-negative PC-3 xenograft tumor growth was not affected by the same formulation in the same way as PSMA-positive tumors growth was not modified by polymeric vehicles.

Control of the initial burst would be a key to extend the total duration of release and is also a prerequisite for the delivery of therapeutics activating the immune system. A small burst could be an advantage to rapidly saturate the tumor receptors and recruit the T cells, but a large burst would induce an uncontrolled activation of the immune system translating into a severe cytokine release syndrome (42). Regarding this study, the promising behavior of the Bij591 polymeric formulations can still be improved in terms of  $C_{max}$  reduction and lower  $C_{max}/C_{ss}$  (steady state concentration) ratio. However, the poor *in vitro/in vivo* correlation (IVIVC) could hamper the optimization of the formulations. The difference of release profiles *in vivo* compared with *in vitro* can probably be explained by several factors: the absence in the release buffer of living cells or enzymes but also the interstitial fluid flow and tissue pressure applied on the depot. All these variables can modify the absorption of the protein as well of the solvent in the subcutaneous area, the rate of the phase inversion and the degradation kinetics of the depot. An interesting add-on to this drug delivery approach would be formulating the drug preencapsulated in particles (43–46). In fact, in the presence of certain excipients, some particles have the convenience to provide a stable microenvironment for the proteins and to be more compatible with *in situ* forming gels than the proteins in terms of hydrophobicity and interactions with the gel copolymers (47–49). Moreover, even if the drug loading capacity of particles are usually lower than *in situ* forming gels, the high specific activity of Bij591 does not require high capacity loading (6%–12% for a 2–4-week delivery, respectively). This combination delivery system, by preserving the particles around the injection site, would also enable the possibility to treat oligo-metastases locally or maintain the bispecific antibody in the postsurgical area to prevent possible local recurrence.

In conclusion, an injectable *in situ* biodegradable polymer-based protein delivery system was successfully designed to prolong the *in vivo* elimination half-life and the therapeutic effect of a small bispecific T-cell engager targeting PSMA in prostate cancer. The polymeric technology preserves the stability and functionality

of the protein and the composition of the polymers can modulate the release profile *in vitro* and *in vivo*. Very encouragingly, a significant decrease in tumor growth was observed in animal models upon the administration of the formulated bispecific antibody. This technology represents a promising therapeutic approach and could be transposed to other cancer types using similar bispecific antibodies scaffolds able to target different tumor markers.

### Disclosure of Potential Conflicts of Interest

N.H. Bander has ownership interest (including stock, patents, etc.) in BZL Biologics, LLC. No potential conflicts of interest were disclosed by the other authors.

### Authors' Contributions

**Conception and design:** W. Leconet, N.H. Bander

**Development of methodology:** W. Leconet, H. Liu, M. Guo, T. Vrlinic, J.S. Batra, S. Grizot, N.H. Bander

**Acquisition of data (provided animals, acquired and managed patients, provided facilities, etc.):** W. Leconet, C. Molinier, M. Oster, J.S. Batra, S. Grizot, N.H. Bander

**Analysis and interpretation of data (e.g., statistical analysis, biostatistics, computational analysis):** W. Leconet, S.L. Lamer-Déchamps, C. Molinier, T. Vrlinic, M. Oster, A.L. Noriega, N.H. Bander

**Writing, review, and/or revision of the manuscript:** W. Leconet, H. Liu, M. Guo, S.L. Lamer-Déchamps, M. Oster, J.S. Batra, A.L. Noriega, S. Grizot, N.H. Bander

**Administrative, technical, or material support (i.e., reporting or organizing data, constructing databases):** W. Leconet, S.L. Lamer-Déchamps, S. Kim, T. Vrlinic, F. Liu, V. Navarro, N.H. Bander

**Study supervision:** W. Leconet, H. Liu, A.L. Noriega, N.H. Bander

### Acknowledgments

The authors wish to thank Dr. Loïc Longeart for histopathology studies assistance. The work described in this publication has been funded with support from MedinCell SA (France) and the WCM Urologic Oncology Research Fund (both granted to N.H. Bander).

The costs of publication of this article were defrayed in part by the payment of page charges. This article must therefore be hereby marked *advertisement* in accordance with 18 U.S.C. Section 1734 solely to indicate this fact.

Received November 15, 2017; revised April 5, 2018; accepted June 4, 2018; published first June 11, 2018.

### References

- Carter P. Improving the efficacy of antibody-based cancer therapies. *Nat Rev Cancer* 2001;1:118–29.
- Weiner GJ. Building better monoclonal antibody-based therapeutics. *Nat Rev Cancer* 2015;15:361–70.
- Yang F, Wen W, Qin W. Bispecific antibodies as a development platform for new concepts and treatment strategies. *Int J Mol Sci* 2016;18:48–69.
- Nagorsen D, Kufer P, Baeuerle PA, Bargou R. Blinatumomab: a historical perspective. *Pharmacol Ther* 2012;136:334–42.
- Bokemeyer C. Catumaxomab–trifunctional anti-EpCAM antibody used to treat malignant ascites. *Expert Opin Biol Ther* 2010;10:1259–69.
- Stieglmaier J, Benjamin J, Nagorsen D. Utilizing the BiTE (bispecific T-cell engager) platform for immunotherapy of cancer. *Expert Opin Biol Ther* 2015;15:1093–9.
- Huehls AM, Coupet TA, Sentman CL. Bispecific T-cell engagers for cancer immunotherapy. *Immunol Cell Biol* 2015;93:290–6.
- Zhu M, Wu B, Brandl C, Johnson J, Wolf A, Chow A, et al. Blinatumomab, a bispecific T-cell engager (BiTE<sup>®</sup>) for CD-19 targeted cancer immunotherapy: clinical pharmacology and its implications. *Clin Pharmacokinet* 2016;55:1271–88.
- Tiwari RV, Patil H, Repka MA. Contribution of hot-melt extrusion technology to advance drug delivery in the 21st century. *Expert Opin Drug Deliv* 2016;13:451–64.
- Schweizer D, Serno T, Goepferich A. Controlled release of therapeutic antibody formats. *Eur J Pharm Biopharm* 2014;88:291–309.
- Agarwal P, Rupenthal ID. Injectable implants for the sustained release of protein and peptide drugs. *Drug Discov Today* 2013;18:337–49.
- Peer D, Karp JM, Hong S, Farokhzad OC, Margalit R, Langer R. Nanocarriers as an emerging platform for cancer therapy. *Nat Nanotechnol* 2007;2:751–60.
- Gohil K. Pharmaceutical approval update. *P T Peer Rev J Formul Manag* 2015;40:106–22.
- Vaishya R, Khurana V, Patel S, Mitra AK. Long-term delivery of protein therapeutics. *Expert Opin Drug Deliv* 2015;12:415–40.
- Thakur RRS, McMillan HL, Jones DS. Solvent induced phase inversion-based *in situ* forming controlled release drug delivery implants. *J Control Release* 2014;176:8–23.
- Al-Tahami K, Oak M, Singh J. Controlled delivery of basal insulin from phase-sensitive polymeric systems after subcutaneous administration: *in vitro* release, stability, biocompatibility, *in vivo* absorption, and bioactivity of insulin. *J Pharm Sci* 2011;100:2161–71.
- Chang DP, Garripelli VK, Rea J, Kelley R, Rajagopal K. Investigation of fragment antibody stability and its release mechanism from poly(Lactide-co-Glycolide)-triacetin depots for sustained-release applications. *J Pharm Sci* 2015;104:3404–17.
- Allen TM, Cullis PR. Drug delivery systems: entering the mainstream. *Science* 2004;303:1818–22.
- Froksjaer S, Otzen DE. Protein drug stability: a formulation challenge. *Nat Rev Drug Discov* 2005;4:298–306.
- Liu H, Moy P, Kim S, Xia Y, Rajasekaran A, Navarro V, et al. Monoclonal antibodies to the extracellular domain of prostate-specific membrane antigen also react with tumor vascular endothelium. *Cancer Res* 1997;57:3629–34.
- Gaudriault G. Biodegradable drug delivery compositions. United States patent US 9023897 B2. 2015 May 05.
- Nanus DM, Milowsky MI, Kostakoglu L, Smith-Jones PM, Vallabha-josula S, Goldsmith SJ, et al. Clinical use of monoclonal antibody Huj591 therapy: targeting prostate specific membrane antigen. *J Urol* 2003;170:S84–8.
- Kung P, Goldstein G, Reinherz EL, Schlossman SF. Monoclonal antibodies defining distinctive human T-cell surface antigens. *Science* 1979;206:347–9.
- Boyman O, Sprent J. The role of interleukin-2 during homeostasis and activation of the immune system. *Nat Rev Immunol* 2012;12:180–90.
- Holliger P, Hudson PJ. Engineered antibody fragments and the rise of single domains. *Nat Biotechnol* 2005;23:1126–36.
- Strohl WR, Strohl LM. Therapeutic antibody engineering: current and future advances driving the strongest growth area in the pharmaceutical industry. 1st ed. New York, NY: Elsevier; 2012.
- Zou J, Chen D, Zong Y, Ye S, Tang J, Meng H, et al. Immunotherapy based on bispecific T-cell engager with hlgG1 Fc sequence as a new therapeutic strategy in multiple myeloma. *Cancer Sci* 2015;106:512–21.
- Liu L, Lam CK, Long V, Widjaja L, Yang Y, Li H, et al. MGD011, a CD19 × CD3 dual-affinity retargeting Bi-specific molecule incorporating extended circulating half-life for the treatment of B-cell malignancies. *Clin Cancer Res* 2017;23:1506–18.
- Root AR, Cao W, Li B, LaPan P, Meade C, Sanford J, et al. Development of PF-06671008, a highly potent anti-P-cadherin/anti-CD3 bispecific DART molecule with extended half-life for the treatment of cancer. *Antibodies* 2016;5:6.
- Unverdorben F, Färber-Schwarz A, Richter F, Hutt M, Kontermann RE. Half-life extension of a single-chain diabody by fusion to domain B of staphylococcal protein A. *Protein Eng Des Sel* 2012;25:81–8.
- Unverdorben F, Hutt M, Seifert O, Kontermann RE. A fab-selective immunoglobulin-binding domain from streptococcal protein G with improved half-life extension properties. *PLoS One* 2015;10:e0139838.

Leconet et al.

32. Hopp J, Hornig N, Zettlitz KA, Schwarz A, Fuss N, Müller D, et al. The effects of affinity and valency of an albumin-binding domain (ABD) on the half-life of a single-chain diabody-ABD fusion protein. *Protein Eng Des Sel* 2010;23:827–34.
33. Hutt M, Färber-Schwarz A, Unverdorben F, Richter F, Kontermann RE. Plasma half-life extension of small recombinant antibodies by fusion to immunoglobulin-binding domains. *J Biol Chem* 2012;287:4462–9.
34. Friedrich M, Raum T, Lutterbues R, Voelkel M, Deegen P, Rau D, et al. Regression of human prostate cancer xenografts in mice by AMG 212/BAY2010112, a novel PSMA/CD3-bispecific BiTE antibody cross-reactive with non-human primate antigens. *Mol Cancer Ther* 2012;11:2664–73.
35. Baum V, Bühler P, Gierschner D, Herchenbach D, Fiala GJ, Schamel WW, et al. Antitumor activities of PSMA×CD3 diabodies by redirected T-cell lysis of prostate cancer cells. *Immunotherapy* 2013;5:27–38.
36. Hernandez-Hoyos G, Sewell T, Bader R, Bannink J, Chenault RA, Daugherty M, et al. MOR209/ES414, a novel bispecific antibody targeting PSMA for the treatment of metastatic castration-resistant prostate cancer. *Mol Cancer Ther* 2016;15:2155–65.
37. Rajagopal K, Wood J, Tran B, Patapoff TW, Nivaggioli T. Trehalose limits BSA aggregation in spray-dried formulations at high temperatures: implications in preparing polymer implants for long-term protein delivery. *J Pharm Sci* 2013;102:2655–66.
38. Maggio ET. Use of excipients to control aggregation in peptide and protein formulations. *J Excip Food Chem* 2010;1:40–9.
39. Chandrashekar G, Udupa N. Biodegradable injectable implant systems for long term drug delivery using poly (lactic-co-glycolic) acid copolymers. *J Pharm Pharmacol* 1996;48:669–74.
40. Graham PD, Brodbeck KJ, McHugh AJ. Phase inversion dynamics of PLGA solutions related to drug delivery. *J Control Release* 1999;58:233–45.
41. Wretling A. The toxicity of low-molecular triglycerides. *Acta Physiol Scand* 1957;40:338–43.
42. Kroschinsky F, Stölzel F, von Bonin S, Beutel G, Kochanek M, Kiehl M, et al. New drugs, new toxicities: severe side effects of modern targeted and immunotherapy of cancer and their management. *Crit Care Lond Engl* 2017;21:89.
43. Arai T, Benny O, Joki T, Menon LG, Machluf M, Abe T, et al. Novel local drug delivery system using thermoreversible gel in combination with polymeric microspheres or liposomes. *Anticancer Res* 2010;30:1057–64.
44. Geng H, Song H, Qi J, Cui D. Sustained release of VEGF from PLGA nanoparticles embedded thermo-sensitive hydrogel in full-thickness porcine bladder acellular matrix. *Nanoscale Res Lett* 2011;6:312.
45. Wang W, Deng L, Xu S, Zhao X, Lv N, Zhang G, et al. A reconstituted "two into one" thermosensitive hydrogel system assembled by drug-loaded amphiphilic copolymer nanoparticles for the local delivery of paclitaxel. *J Mater Chem B* 2012;1:552–63.
46. Alizadeh B, Bahari Javan N, Akbari Javar H, Khoshayand MR, Dorkoosh F. Prolonged injectable formulation of Nafarelin using *in situ* gel combination delivery system. *Pharm Dev Technol* 2018;23:132–44.
47. Zhu G, Mallery SR, Schwendeman SP. Stabilization of proteins encapsulated in injectable poly (lactide-co-glycolide). *Nat Biotechnol* 2000;18:52–7.
48. Ma G. Microencapsulation of protein drugs for drug delivery: strategy, preparation, and applications. *J Control Release* 2014;193:324–40.
49. Yu M, Wu J, Shi J, Farokhzad OC. Nanotechnology for protein delivery: overview and perspectives. *J Control Release* 2016;240:24–37.

# Molecular Cancer Therapeutics

## Anti-PSMA/CD3 Bispecific Antibody Delivery and Antitumor Activity Using a Polymeric Depot Formulation

Wilhem Leconet, He Liu, Ming Guo, et al.

*Mol Cancer Ther* 2018;17:1927-1940. Published OnlineFirst June 11, 2018.

**Updated version** Access the most recent version of this article at:  
doi:[10.1158/1535-7163.MCT-17-1138](https://doi.org/10.1158/1535-7163.MCT-17-1138)

**Supplementary Material** Access the most recent supplemental material at:  
<http://mct.aacrjournals.org/content/suppl/2018/06/09/1535-7163.MCT-17-1138.DC1>

**Cited articles** This article cites 47 articles, 8 of which you can access for free at:  
<http://mct.aacrjournals.org/content/17/9/1927.full#ref-list-1>

**E-mail alerts** [Sign up to receive free email-alerts](#) related to this article or journal.

**Reprints and Subscriptions** To order reprints of this article or to subscribe to the journal, contact the AACR Publications Department at [pubs@aacr.org](mailto:pubs@aacr.org).

**Permissions** To request permission to re-use all or part of this article, use this link  
<http://mct.aacrjournals.org/content/17/9/1927>.  
Click on "Request Permissions" which will take you to the Copyright Clearance Center's (CCC) Rightslink site.